

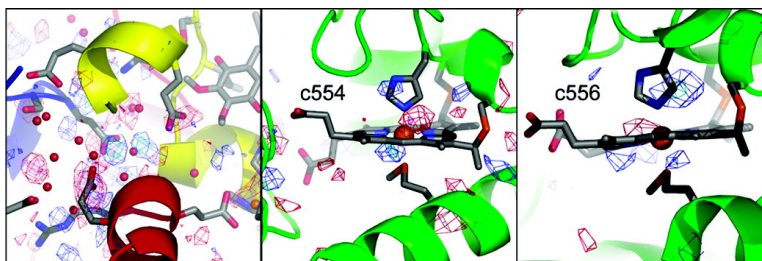
Communication

## Specific Radiation Damage Illustrates Light-Induced Structural Changes in the Photosynthetic Reaction Center

Richard H. G. Baxter, Brandon-Luke Seagle, Nina Ponomarenko, and James R. Norris

*J. Am. Chem. Soc.*, **2004**, 126 (51), 16728-16729 • DOI: 10.1021/ja0448115 • Publication Date (Web): 04 December 2004

Downloaded from <http://pubs.acs.org> on April 5, 2009



### More About This Article

Additional resources and features associated with this article are available within the HTML version:

- Supporting Information
- Links to the 2 articles that cite this article, as of the time of this article download
- Access to high resolution figures
- Links to articles and content related to this article
- Copyright permission to reproduce figures and/or text from this article

[View the Full Text HTML](#)

## Specific Radiation Damage Illustrates Light-Induced Structural Changes in the Photosynthetic Reaction Center

Richard H. G. Baxter,<sup>\*,†</sup> Brandon-Luke Seagle, Nina Ponomarenko, and James R. Norris

Department of Chemistry, University of Chicago, 5735 South Ellis Avenue, Chicago, Illinois 60637

Received August 27, 2004; E-mail: rbaxter@alumni.uchicago.edu

The photosynthetic reaction center of the purple non-sulfur bacterium *Blastochloris viridis* was the first integral membrane protein whose structure was determined to atomic resolution.<sup>1</sup> Upon excitation by light, an electron is donated by a special pair (P) of bacteriochlorophyll molecules, eventually arriving at the terminal electron acceptor Q<sub>B</sub>. The special pair is rereduced by a set of four hemes within a tightly bound cytochrome subunit, which are distinguished by their absorption maxima and redox potentials. The order of proximity for the four hemes is: P, c<sub>559</sub> (+380 mV), c<sub>552</sub> (+20 mV), c<sub>556</sub> (+320 mV), c<sub>554</sub> (−60 mV).<sup>2</sup>

We have previously used time-resolved crystallography to investigate a proposed structural change in the *B. viridis* reaction center.<sup>3</sup> No large-scale motions were apparent in the experimental difference Fourier map; in particular, no motion of the secondary acceptor Q<sub>B</sub> was observed. To test this result further, a freeze-trapping experiment has been performed in *B. viridis*. While the position of Q<sub>B</sub> is unchanged, difference Fourier maps do show significant changes correlated to cofactor function.

Reaction centers were prepared as previously described.<sup>3</sup> No specific chemical oxidation or reduction was performed during purification so as to alter the redox state of the bound cytochrome. Absorption spectra (Figure S1) show that all but the highest potential heme (c<sub>559</sub>) are mostly oxidized. Reaction centers were crystallized under standard conditions<sup>4</sup> and transiently soaked in a sucrose cryobuffer similar to that previously used to freeze crystals for EPR analysis.<sup>5</sup>

Three datasets were measured from two crystals. The first crystal was frozen in darkness and a dataset collected, and then a further dataset was collected under continuous illumination at 100 K. This illumination regime should probe the state c<sub>559</sub><sup>+</sup>Q<sub>A</sub><sup>−</sup>, since electron transfer to Q<sub>B</sub> does not occur for samples frozen in darkness.<sup>6</sup> The second crystal was illuminated with a single flash from a Xenon flash lamp and immediately frozen, and then a dataset was collected in the dark. This crystal should exist in the charge-separated state during freezing, as charge recombination of the c<sub>559</sub><sup>+</sup>Q<sub>B</sub><sup>−</sup> state is slow.<sup>7</sup> Since charge recombination can still occur at 100 K, however, data collection should probe the charge-neutral state.

The dark dataset was collected from 90 images with 5-s exposure per image, the low-temperature illumination dataset from a further 90 images with 20-s exposure per image, and the flash-freeze dataset collected from 135 images with 30 s per image. The radiation dose for the dark dataset was estimated by the program RADDOS<sup>8</sup> to be 8 × 10<sup>5</sup> Gy with the ratio of doses in the three datasets being 1:5:9.

Figure 1 shows the difference Fourier map for the first crystal (low-temperature illumination). While it is not possible to compare the absolute scale of different maps, all had maximum and minimum electron density ratios similar to the rms electron density ratio of

6:1, with the exception of the difference map for low-temperature illumination (Figure 1b), whose strongest features extend to −9σ.

The significant differences observed in Figure 1b are the result of radiation damage. This damage is not distributed evenly throughout the protein, however, but localized on specific susceptible groups.<sup>10</sup> The most significant features in the difference between the dark and low-temperature illuminated dataset lie in a cluster at the interface of the L, M, and H subunits (Figure S2), between the Q<sub>B</sub> site and the protein surface where a channel of ordered water leads from the Q<sub>B</sub> site to the cytoplasm.<sup>10</sup> In particular, a −9σ peak occurs to Glu M234, which occupies a position in *B. viridis* similar to Glu H122 in the *Rhodobacter sphaeroides* RC, at the bifurcation point of the water channel. Electrostatic calculations in *B. viridis* suggest that a cluster of glutamic acid residues including Glu M234 contains 1 to 2 protons in the pH range 5–11.<sup>11</sup> Hence, the susceptibility of Glu M234 to radiation damage illustrates its position of physiological relevance for proton transfer to Q<sub>B</sub>.

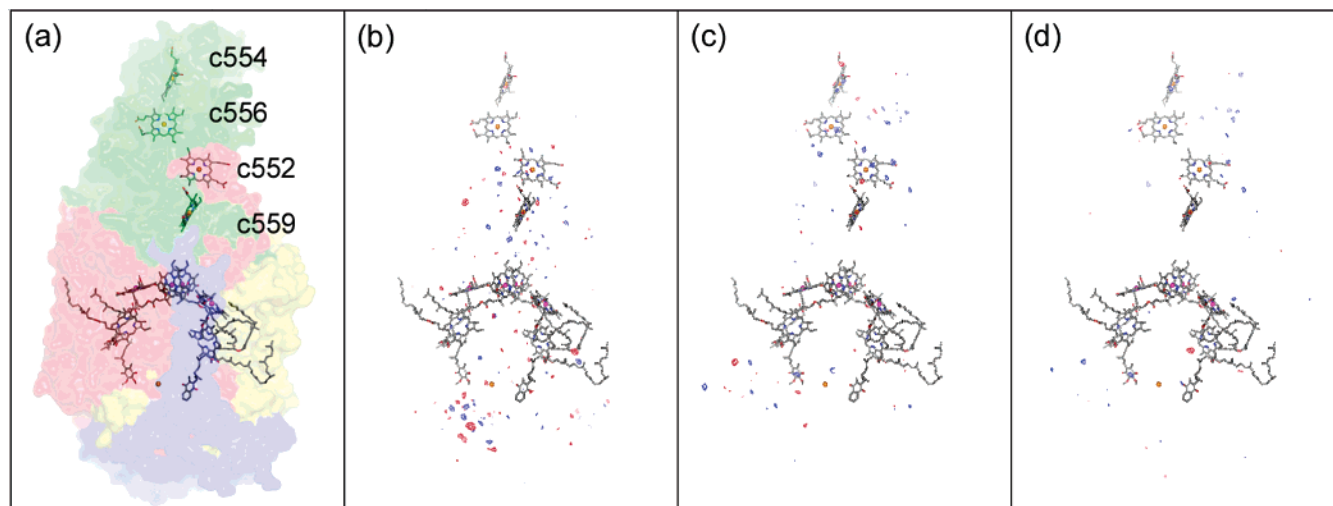
The difference Fourier map for the flash-frozen crystal is qualitatively different to both the dark and low-temperature illumination datasets (Figure 1c,d). This reflects the lower resolution of the flash-frozen dataset and the systematic and random errors between the two crystals. The most significant difference between the low-temperature illumination and the freeze-trapping difference Fourier map is that, in the flash-frozen crystal, the damage in the water channel to Q<sub>B</sub> is much reduced in magnitude relative to specific changes observed on the two distal hemes. This difference is retained, albeit at lower magnitude, in the difference between the two light datasets (Figure 1d). However, an inverse of differences observed in Figure 1b is not observed in Figure 1d.

Figure 2 shows the nature of the specific damage to the hemes. Three features are seen at 5σ on the two most distal hemes, c<sub>554</sub> and c<sub>556</sub>, a negative feature adjacent to the iron, and positive features on the proximal histidine ligand and on the distal side of the porphyrin ring.

We propose that these changes are due to radiation-induced reduction of the distal hemes, which causes a small rearrangement due to strengthening of the Met-Fe bond.<sup>12</sup> The two distal hemes, which have solution midpoint potentials of −60 mV (c<sub>554</sub>) and 320 mV (c<sub>556</sub>), were both initially oxidized. The highest potential heme c<sub>559</sub> is reduced in the sample, and hence no features are seen; although reduction of the low potential heme c<sub>552</sub> may occur, its proximal and distal ligands are identical, and thus no overall rearrangement is observed.

Why is the distribution of radiation damage different between the flash-frozen crystal and that collected under low temperature illumination? Although they may merely be artifacts of the lower resolution in the flash-frozen dataset, we believe the differences reflect the reorganization of protein and ordered water in the protein to accommodate the appearance of a negative charge at Q<sub>B</sub>. Such reorganization is free to occur in the second crystal that exists in

<sup>†</sup> Present address: Howard Hughes Medical Institute Research Laboratories, University of Texas Southwestern Medical Center at Dallas, Dallas TX 75390-9050.



**Figure 1.** (a) Protein surface of PRC colored by subunits C (green), L (yellow), M (red) and H (blue), and cofactors. Difference Fourier maps for (b) low-temperature illumination vs dark, (c) flash-frozen vs dark, and (d) flash-frozen vs low-temperature illumination. Number of reflections in common: 87,826 (dark and low temp. illum.), 43,991 (dark and flash-freeze) and 42,625 (low temp. illum. and flash-freeze). Phases obtained from a model following simulated annealing and deletion of atoms near significant features. Difference amplitudes weighted by their relative error.<sup>9</sup>

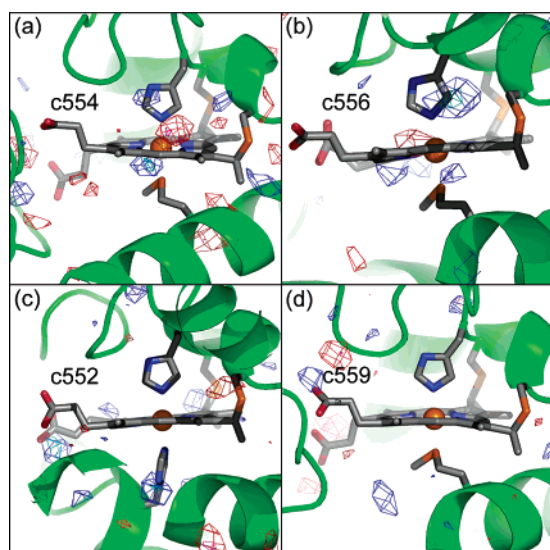


**Figure 2.** Difference Fourier map of the four hemes within the cytochrome subunit for the flash-frozen dataset. Contours at  $\pm 3.5\sigma$  (red -ve, blue +ve) and  $\pm 5\sigma$  (magenta -ve, cyan +ve).

the charge-separated state prior to freezing but not in the first crystal that was frozen prior to generation of the charge-separated state. Specifically, the protons in the acidic cluster, which may be converted into hydrogen atom radicals by the X-ray beam, are redistributed in the charge-separated state toward the  $Q_B$  site.

In the absence of a large motion accompanying electron transfer from  $Q_A$  to  $Q_B$ ,<sup>3,13</sup> the rearrangement of acidic residues in response to the appearance of negative charge on  $Q_A$  is a plausible “conformational gate”.<sup>14</sup> Future studies of crystals frozen under conditions to specifically poise the cytochrome subunit in different redox states and collection of data with specific radiation doses

will allow more accurate determination of the extent of structural rearrangements due to electron transfer within this biological system.

**Acknowledgment.** This work was funded by DOE Grant DE-FG02-96ER14675 to J.R.N., Burroughs Wellcome Fellowship 1001774 to R.H.G.B., and a Richter Fund summer research scholarship to B.S. Keith Moffat and Jason Key are thanked for many fruitful discussions, and Phoebe Rice and Xiaojing Yang, for assistance in establishing freezing conditions.

**Supporting Information Available:** UV/vis absorption spectra of purified RCs, X-ray data processing statistics, and additional difference Fourier maps. This material is available free of charge via the Internet at <http://pubs.acs.org>.

## References

- (1) Deisenhofer, J.; Epp, O.; Miki, K.; Huber, R.; Michel, H. *Nature* **1985**, *318*, 618–624.
- (2) Nitschke, W.; Dracheva, S. M. In *Anoxygenic Photosynthetic Bacteria*; Blankenship, R. E., Madigan, M. T., Bauer, C. E., Eds.; Kluwer Academic Publishers: Dordrecht, Boston, 1995; pp 775–805.
- (3) Baxter, R. H.; Ponomarenko, N.; Srajer, V.; Pahl, R.; Moffat, K.; Norris, J. R. *Proc. Natl. Acad. Sci. U.S.A.* **2004**, *101*, 5982–5987.
- (4) Michel, H. *J. Mol. Biol.* **1982**, *158*, 567–572.
- (5) Gast, P.; Wasielewski, M. R.; Schiffer, M.; Norris, J. R. *Nature* **1983**, *305*, 451–452.
- (6) Kleinfeld, D.; Okamura, M. Y.; Feher, G. *Biochemistry* **1984**, *23*, 5780–5786.
- (7) Shopes, R. J.; Wraight, C. A. *Biochim. Biophys. Acta* **1985**, *806*, 348–356.
- (8) Murray, J. W.; Garman, E. F.; Ravelli, R. B. *J. Appl. Crystallogr.* **2004**, *37*, 513–522.
- (9) Ursby, T.; Bourgeois, D. *Acta Crystallogr.* **2004**, *A53*, 564–575.
- (10) Ravelli, R. B.; McSweeney, S. M. *Structure* **2000**, *8*, 315–28.
- (11) Lancaster, C. R. D.; Michel, H.; Honig, B.; Gunner, M. R. *Biophys. J.* **1996**, *70*, 2469–2492.
- (12) Moore, G. R.; Pettigrew, G. W., *Cytochromes c: evolutionary, structural, and physicochemical aspects*; Springer-Verlag: New York, 1990.
- (13) Remy, A.; Gerwert, K. *Nat. Struct. Biol.* **2003**, *10*, 637–644.
- (14) Mulikjanian, A. Y. *FEBS Lett.* **1999**, *463*, 199–204.

JA0448115